Analysis of Short and Long Crack Behavior and Single Overload Effect by Crack Opening Stress

Sam-Hong Song* and Kyeong-Ro Lee**

(Received August 28, 1998)

The study analyzed the behaviors of short and long crack as well as the effect of single tensile overload on the crack behaviors by using fatigue crack opening behavior. Crack opening stress is measured by an elastic compliance method which may precisely and continuously provide many data using strain gages during experiment. The unusual growth behaviors of short crack and crack after the single tensile overload applied, was explained by the variations of crack opening stress. In addition, fatigue crack growth rate was expressed as a linear form for short crack as for long crack by using effective stress intensity factor range as fracture mechanical parameter, which is based on crack closure concept. And investigation is performed with respect to the relation between plastic zone size formed at the crack tip and crack retardation, crack length and the number of cycles promoted or retarded, and the overload effect on the fatigue life.

Key Words : Short Crack, Long Crack, Single Overload, Crack Opening Stress, Effective Stress Range Ratio, Effective Stress Intensity Factor Range

1. Introduction

Short crack is a crack to which LEFM is not applicable and propagates faster relatively than long crack, so that if the data about long crack is applied to a short crack, the fatigue life would be overestimated. These are due to local plasticity, micro-metal structure, crack tip environment, propagation mechanism, crack driving force, crack closure, etc. (Suresh and Ritchie, 1984). No elasto-plastic analysis on short crack behavior can be deduced without introducing crack closure effect (Suresh and Ritchie, 1984). Previous researches of short crack include the behavior of crack initiation due to hardness difference of microstructure (Yamada et al., 1987), the phenomenon of crack arrest, theoretical approach to short crack growing from defects (Perez et al., 1990), and so on. Systematic fracture mechanics estimation, however, on short crack through test and theoretical equations has not yet been accom-plished due to experimental difficulties. In this study, thus, short crack behavior which would provide significant data for fatigue life prediction is quantitatively evaluated through experimental measurements of crack opening stress and the application of fracture mechanics parameter to the results.

The study on fatigue life under variable loading is an important subject for fatigue life prediction and safe design; especially the study on single tensile overload, which would provide fundamental data for the effect of variable loading, has been continuously performed because of its importance. When researches on overload are analyzed, most of results are that crack growth is retarded after overload (Gan and Weertman, 1983), but there are some contradictory results that crack growth is retarded after acceleration or accelerated according to the test condition and the mode of loading (Song and Won, 1985). While the effects of overload on fatigue life design are important factors, the results are differently expressed. Also, most of former researches considered the effect of overload with respect to long crack, but there is not many researches on overload with respect to short crack due to exper-

* Professor, Dept. of Mechanical Engineering, Korea University, Seoul, Korea
** Professor, Faculty of Automobile, Shinsung College, Chungnam, Korea

imental difficulties. Because short crack propagates faster than long crack under the same LEFM parameter, and growth mechanism is very different from long crack, examination of the effect of overload with respect to short crack would provide important data for fatigue life prediction of mechanical structures or components.

Meanwhile, the employment of effective stress intensity factor considering crack closure behavior makes nonlinear crack behavior analysis possible, and many researches have been performed. Measurement methods on crack closure behavior divide into direct measurement method and indirect method. The direct measurement methods include the method using SEM, replica method, laser interferometric strain/displacement gage method. Among the indirect measurement methods are the one using clip gage or strain gage (Elber, 1971 ; Park et al., 1998), and ultrasonic method. Direct method measures precise crack opening point of crack tip. but due to time consuming, it is hard to obtain enough data and the test machine should be stopped or loading rate should be very slow in measuring. Also, ultrasonic method is not sufficiently as exact as strain gage or clip gage method. Thus, crack opening stresses are measured by elastic compliance method using strain gages, which can precisely and continuously collect many data during test, and the characteristic of short crack and the effects of single tensile overload are analyzed by crack opening behavior.

2. Specimen and Test Method

Cr-Mo steel alloy. SA-387 is employed as specimen material and its chemical composition and mechanical properties are listed in Table 1, and Table 2 respectively.

Two types of specimen with hole defect of 0.5 mm diameter, depth (H specimen) and pre-cracked smooth specimen (P specimen) are used. Figure 1 shows the geometry where crack length a is defined as the half of total crack length $2a$, and crack length is measured by micro-scope after stopping the test machine. The micro-scope

of 140 magnification factor is used when crack length is long, and 280 when crack length is short. Crack length is measured about 80 times until specimen failure, and each measurement takes approximately 30 seconds. The pre-cracked smooth specimen(P specimen) manufacturing process is shown in Fig. 2. P specimen is manufactured to examine short crack behavior not effected by stress concentration, in the way after drilling a hole defect of 0.3 mm diameter and 0.1 mm depth. initiating fatigue crack from hole and then removing hole defect. The specimen surface is abraded by emery paper and alumina of which particle size is about 0.3 μm. Also, a hole defect is drilled by using micro-scope and dial-gage with 1/1000 mm scale.

Many researchers (Elber, 1971 ; Kurihara et al., 1987 ; Schijve, 1981) examined that opening ratio, U changes dependently on stress ratio, R, and the relation equations have been proposed. Also, the effect of overload with R variation was studied (Stephens et al., 1976). In this paper, however, short crack and long crack behaviors are investigated and the effects of a single overload on

Table 1 Chemical composition

Material	Composition (Weight percent)						
	C	Si	Mn	P	S	Cr	Mo
SA-387	0.12	0.55	0.53	0.007	0.005	1.40	0.55

Table 2 Mechanical properties

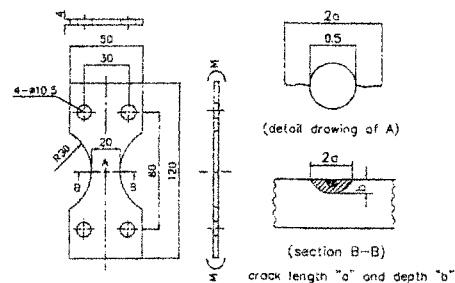| Yield strength (MPa)	Ultimate strength (MPa)	Elonga-tion (%)	Elasticity Modulus (MPa)	Poisson's ratio
350	585	24	191200	0.28

Fig. 1 Geometries of fatigue test specimen

(a) Cross section of specimen
with micro hole defect

(b) Fatigue crack growth from
the micro hole defect

(c) Remove micro hole defect
by abrasive paper

(d) Smooth plate specimen
with pre-crack

(a′) Cross section of specimen
with micro hole defect

(b′) Fatigue crack growth from
the micro hole defect

(d′) Smooth plate specimen
with pre-crack
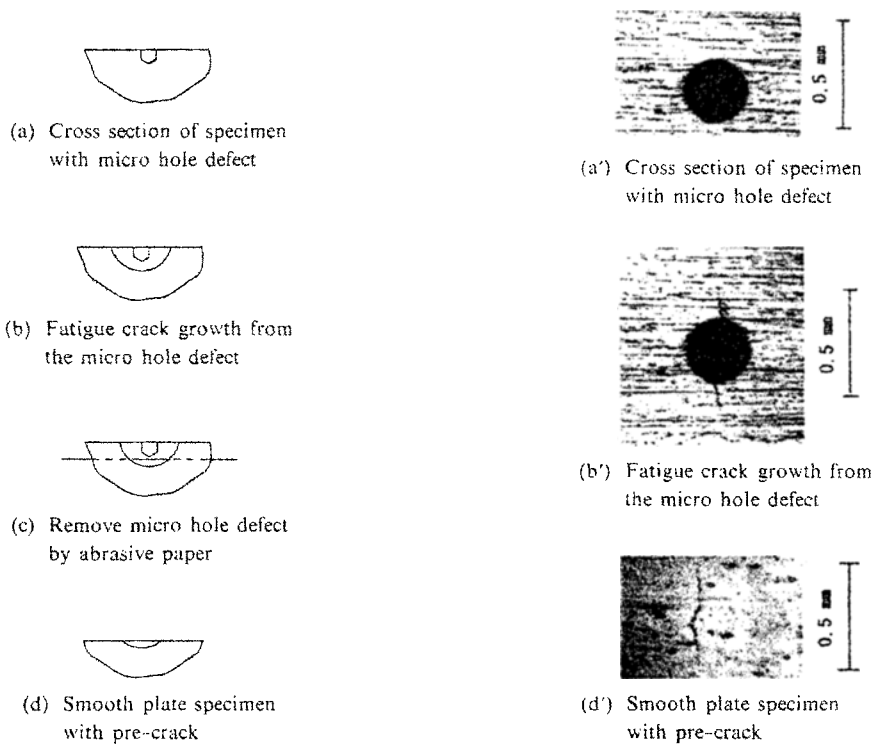
Fig. 2 Manufacturing process of the pre-cracked smooth specimen (P specimen)

$2\sigma_{max}=334MPa$
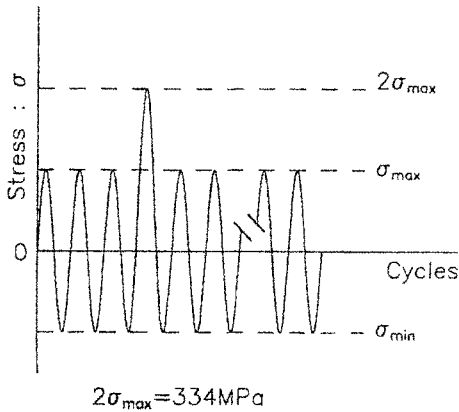
Fig. 3 Schematic representation of stress history

crack behavior are examined, so the relative variations of U are focused and stress ratio R is held constant. Because σ_{op} approaches to "0" from the experimental results, R in the range of "+", makes it difficult to exactly measure opening stress. Therefore, compressive load is needed to observe opening stress exactly, and then R is held -1. Also, it is not easy to experiment tension-compression test in case of $R=-1$ so that

out of plane bending load is applied for experiment. Figure 3 shows stress history, where the single overload is 2 times as large as the maximum load. The short crack range is found through tests. and then the effects of the single overload on short and long crack are analyzed by crack opening behavior.

Crack opening stresses are measured by elastic compliance method using two $120 \, \Omega$ strain gages : one (gage A) was 20 mm away from the crack or hole defect, and the other (gage B) was attached possibly close to the crack or hole defect. Gage A measured the displacement produced by external load while gage B measured it considering opening and closure of the crack. In other words, gage A measured external load and gage B measured the load considering opening and closure of the crack. by which crack opening stress was measured. Figure 4 showed strain gages attached to the specimen. While gage A was 1.0mm in length. gage B was 0.3mm in length that enables to detect small variation of displacement. Figure 5 shows the picture of gage B attached to
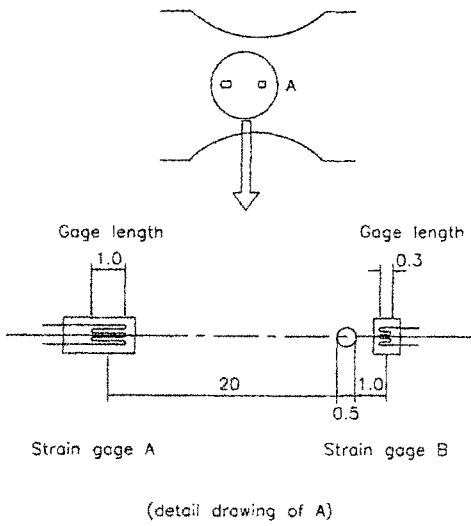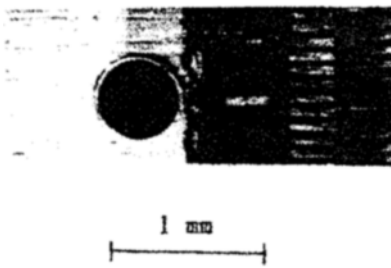
Fig. 4   Strain gages on the H specimen

Fig. 5   (a) Strain gage B on the P specimen
         (b) Strain gage B on the H specimen

P and H specimen.

Figure 6 shows the flow of processing data collected from strain gage. The resistance variation from strain gage converts to the variation of
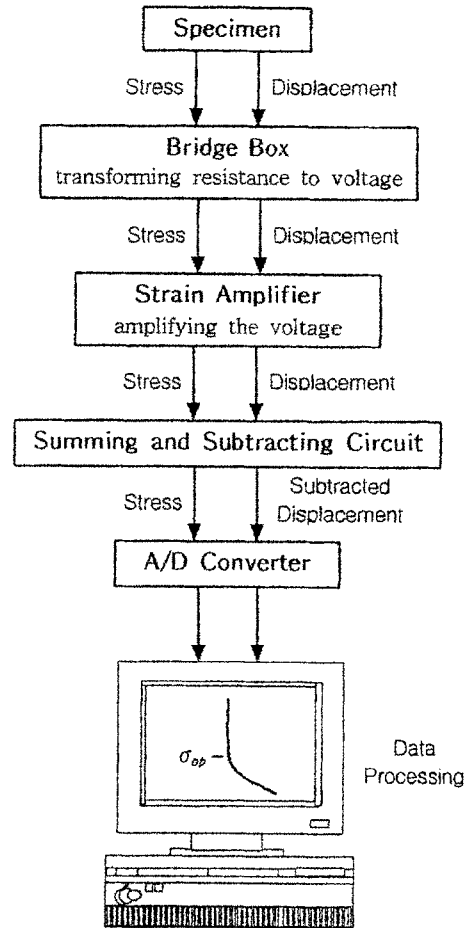

Fig. 6   Schematic diagram of data processing

voltage after going through bridge box, and then it gets into summing and subtracting circuit via strain amplifier. The signals of load and displacement are changed by 3 variable resistors to appropriate slope and magnitude then passed to A/D converter. The input signal in A/D converter is translated by program and graphed on monitor. All devices are grounded to prevent noises to signal.

3. Test Results and Discussions

3.1 Growth behaviors of short crack and long crack

Figure 7 shows the relation between crack propagation rate, da/dN and crack length, a in P and H specimen. As shown, short crack propa-
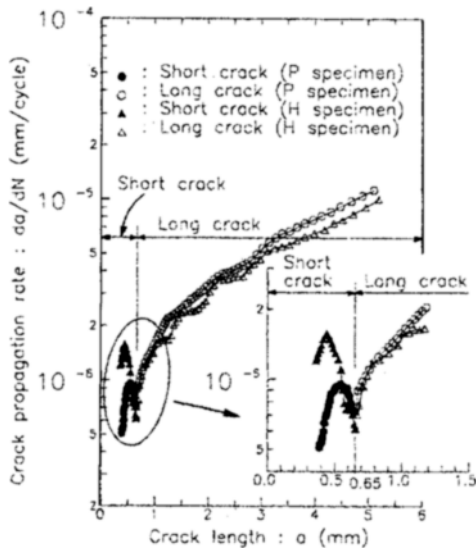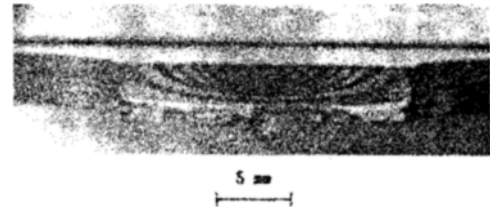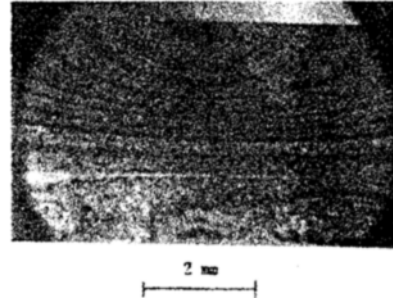
Fig. 7 Relation between crack propagation rate and crack length about P and H specimen at R = −1, σ_{max} = 167 MPa

(a) Beach-marked cross section of the P specimen

(b) Enlarged photo. of (a)

Fig. 8 Fatigue crack shape of the P specimen

gates faster than long crack under the same LEFM parameters. Crack length, a is a main factor to decide LEFM parameters, where as crack length increases, crack propagation rate proportionally increases, but there is a range where the contrary phenomenon occurs, which reveals short crack behavior. In case of P specimen, at crack length, a=0.58 mm, the propagation rate, da/dN is 9.2×10^{-7} mm/cycle, which is faster than the propagation rate, 7.3×10^{-7} mm/cycle at crack length, a=0.65 mm and about the same value as the propagation rate, 9.3×10^{-7} mm/cycle at crack length, a=0.70 mm. Also, in case of H specimen, at crack length, a=0.44 mm, da/dN is 1.57×10^{-6} mm/cycle, which is faster than the propagation rate, 6.12×10^{-7} mm/cycle at crack length, a=0.65 mm and much the same value as the propagation rate, 1.58×10^{-6} mm/cycle at crack length, a=1.02 mm. These short crack behaviors are dominant to the crack length, a=0.65 mm in both of P specimen and H specimen. Also short crack characteristics are greater in H specimen than in P specimen, which is estimated due to the effect of stress field around hole defect (Song and Kim, 1995). Therefore, in order to examine the pure short crack behavior, P

specimen is used which is removed of the initial hole defect to avoid stress concentration.

The relation between crack propagation rate, da/dN and stress intensity factor range, ΔK was defined by the Paris' equation (1) with utilizing Eq. (2) for stress intensity factor, K as proposed by Newman (ASTM-E740, 1988). In this equation, each of G, Φ, S, H is a function of crack length, a, crack depth, b, and specimen thickness, t. Beach marking method was used to identify the relationship between crack length and crack depth which was an essential factor of Newman's formula. Figure 8 shows the temper colored picture of fatigue crack shape of the P specimen obtained by beach marking method.

$$\frac{da}{dN} = C(\Delta K)^m \tag{1}$$

$$K = (G/\Phi) SH \, \sigma \sqrt{\pi a} \tag{2}$$

First, the long crack behavior is examined to investigate the short crack behavior compared with the long crack behavior. In Fig. 9, ΔK is plotted versus da/dN in log-log scale showing the test result performed to examine long crack behavior and threshold stress intensity factor range, ΔK_{th}. The tests are carried out as recom-
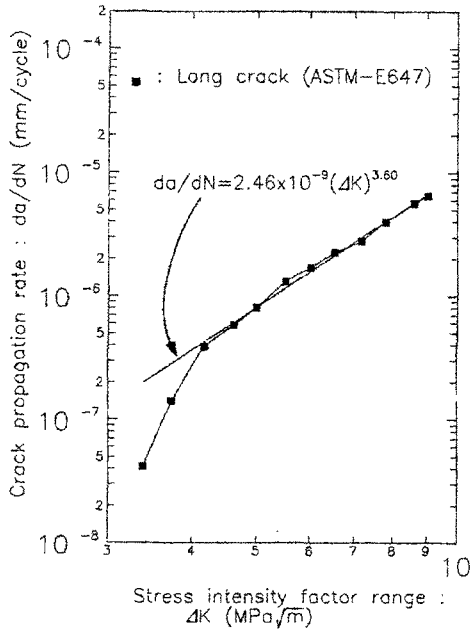
Fig. 9 Relation between crack propagation rate and stress intensity factor range about long crack at R = −1

Fig. 10 Relation between crack propagation rate and stress intensity factor range about short crack and long crack at R = −1

mended in ASTM-E647 (1991). As shown in Fig. 9 and from Eq. (1), ΔK_{th} is about 3 $MPa\sqrt{m}$, where material constants, C and m are 2.46 $\times 10^{-9}$ and 3.60 respectively.

The short crack and long crack behaviors of P specimen are compared in Fig. 10. As pointed out in Fig. 7, the short crack behavior is shown. When the stress intensity factor range, ΔK is 4.2 and 4.6 MPa, the crack propagation rate, da/dN is 3.9×10^{-7} and $5.7 \times 10^{-7} mm/cycle$ respectively in long crack, and 7.3×10^{-7}, $9.3 \times 10^{-7} mm/cycle$ respectively in short crack. In other words, short crack reveals the faster crack propagation rate than that of long crack under the same LEFM parameters (stress intensity factor range). The problems of defining the short crack by the LEFM are the effects of local plastic zone, micro metal structure, crack tip environment, growth mechanism, driving force, crack closure, and so on. This behavior of short crack can not be explained without the introduction of crack closure effect (Suresh and Ritchie, 1984), so that the short crack behavior is to be analyzed by using crack closure behaviors.
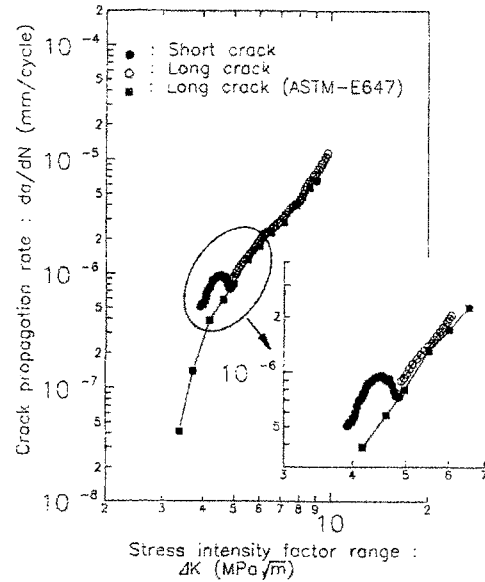
3.2 Analysis of short crack and long crack growth by using crack opening stress

Crack opening stress is the value of applied stress by external load at which the crack tip just starts to open. In other words, the minimum stress at which crack opens during one cycle in fatigue loading and closely related to crack closure. Several factors affecting crack closure are classified as follows (McEvily, 1988).

(1) Plasticity induced closure (Elber, 1971)
(2) Roughness induced closure
(3) Crack filling closure
(4) Phase transformation induced closure
(5) Grain boundary closure (Yamada et al., 1987)

Several models inducing crack closure are not independent, complicatedly correlated. Plasticity-induced closure is the most general model explaining crack closure behavior and expatiates crack growth behavior. Though the other factors have complex effects on crack behavior, the effect of them occurs greatly in some specific cases. For instance, roughness induced closure has great effect when the crack growth is Mode Ⅱ, and crack filling closure has significant effect in high temperature or vacuum environment. Thus, the
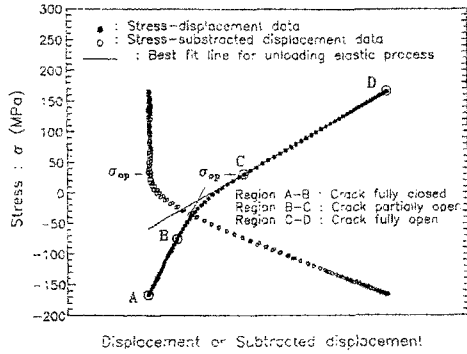
Fig. 11 Example of crack opening stress measurement and schematic stress–displacement curve showing three different regions of specimen compliance

crack closure is explained based on the plasticity induced closure model.

As a fracture mechanics parameter, effective stress intensity factor range, ΔK_{eff} is used and defined as follows :

$$\Delta K_{eff} = K_{max} - K_{op} \tag{3}$$

$$\Delta K_{eff} = U \, \Delta K \tag{4}$$

where U is opening ratio or effective stress range ratio, and defined as follows :

$$U = \frac{\Delta K_{eff}}{\Delta K} = \frac{K_{max} - K_{op}}{K_{max}} = \frac{\sigma_{max} - \sigma_{op}}{\sigma_{max}} \tag{5}$$

σ_{op} : crack opening stress

K_{op} : crack opening stress intensity factor

Stress–displacement and stress–subtracted displacement are plotted in Fig. 11. Stress–subtracted displacement curve (represented by ○) is obtained by subtracting unloading elastic line from stress–displacement curve (represented by ●). The testing machine was 33 Hz of speed and dealt with more than 200 data per cycle to find point of σ_{op}.

In Fig. 12, a plot of stress versus subtracted displacement is shown in short crack range (until crack length, a becomes about 0.65 mm). Figure 13 shows a plot of stress–subtracted displacement from which U is constantly about 0.8 independent of crack length in the range of long crack (when crack length, a is greater than 0.65 mm). However, effective stress range ratio, U of short crack is greater than 0.8 as shown in Fig. 12. This phenomenon means that the specific short crack
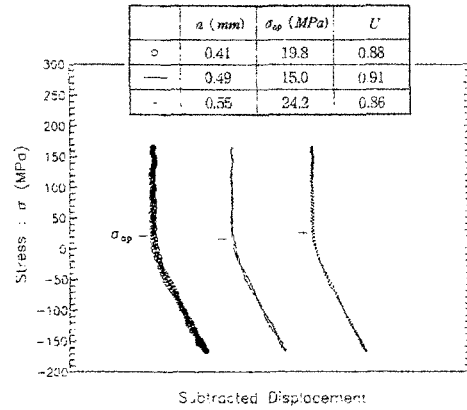

	a (mm)	σ_{op} (MPa)	U
○	0.41	19.8	0.88
—	0.49	15.0	0.91
·	0.55	24.2	0.86

Fig. 12 Relation between stress and subtracted displacement at R = −1, σ_{max} = 167MPa in the range of short crack ($a < 0.65$ mm)

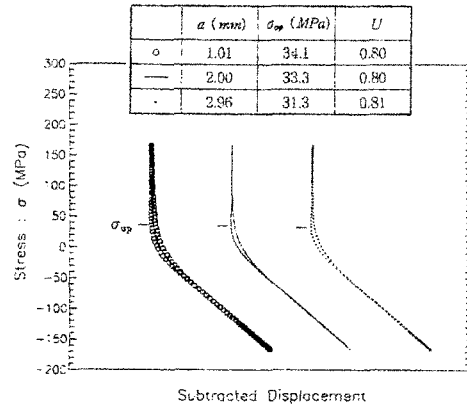|	a (mm)	σ_{op} (MPa)	U
○	1.01	34.1	0.80
—	2.00	33.3	0.80
·	2.96	31.3	0.81

Fig. 13 Relation between stress and subtracted displacement at R = −1, σ_{max} = 167 MPa in the range of long crack ($a > 0.65$ mm)

behavior shown in Fig. 10 can be explained by crack closure behavior. In other words, Eq. (5) means that when U is great, σ_{op} is small in case of the same σ_{max}, and as much the stress range has a greater effects on crack growth. It shows that crack growth rate of short crack is faster than that of long crack under the same ΔK as shown in Fig. 10.

Figure 14 shows a plot of effective stress range ratio, U versus crack length, a, where U decreases until the crack length, a becomes 0.65 mm and then approaches to about 0.8. It can be explained by crack closure concept that U of short crack is greater than that of long crack

(Elber, 1971). In other words, since residual plastic strain formed along the wake of long crack is greater than that of short crack, long crack closes faster than short crack after removing the

Fig. 14 Relation between effective stress range ratio and crack length about P specimen at R= −1, σ_{max}=167 MPa

Fig. 15 Relation between crack propagation rate and effective stress intensity factor range about P specimen at R= −1, σ_{max}=167 MPa

load, and accordingly σ_{op} of long crack is greater than that of short crack, and U is smaller.

Figure 15 shows a plot of crack propagation rate, da/dN versus effective stress intensity factor range, ΔK_{eff}, where solid mark ($\bullet$) represents short crack and open mark ($\circ$) means long crack. All of data points of short crack and long crack fall in a narrow bandwidth and are linearly plotted so that Eq. (1) can be rearranged by using ΔK_{eff} into Eq. (6). In this study, C' is 8.38×10^{-9} and m' is 3.41.

$$\frac{da}{dN}=C'(\Delta K_{eff})^{m'} \qquad (6)$$

3.3 Crack growth behavior after the single overload

In this section, the crack growth characteristics are examined in short crack range and long crack range after a single overload and H specimen is used. In Fig. 7, short crack region is to crack length, a=0.65 mm. When crack length, a is 0.58 mm in case of short crack and a is 1.61 mm and 3.20 mm in case of long crack, the 100 % single overload is applied and the effects on crack growth behavior are examined.
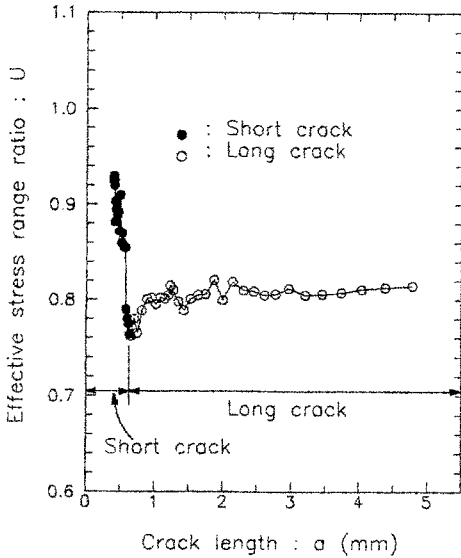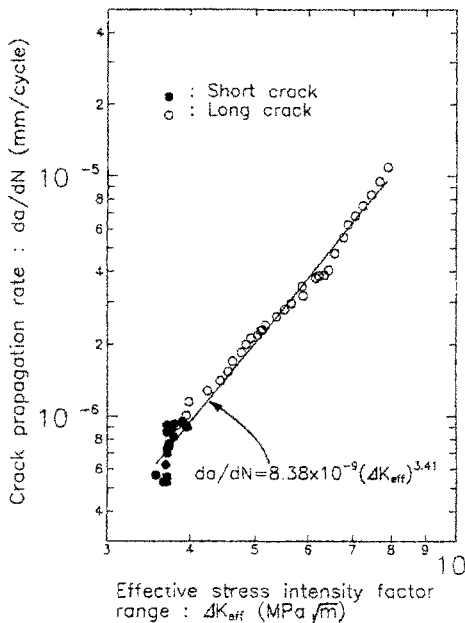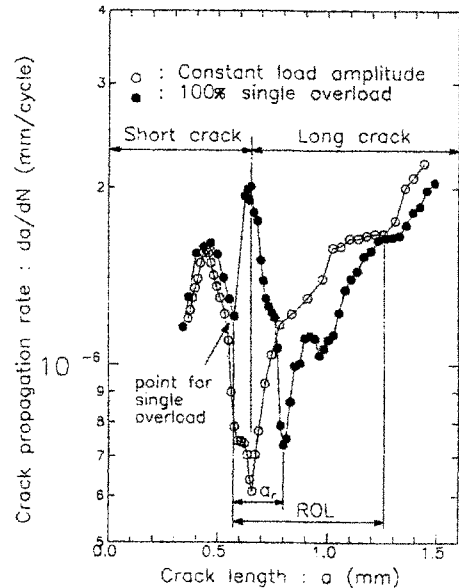
Figure 16 shows curves of da/dN versus a,

Fig. 16 Comparison of crack propagation rate for constant load amplitude and 100 % single overload applied at a=0.58 mm

where single overload is applied, when crack length a is 0.58 *mm*. Open mark (○) represents crack growth behavior under constant amplitude loading and solid mark (●) represents crack growth behavior when 100 % single overload is applied. Under constant amplitude loading, as crack length a increases to 0.58, 0.65, 0.79, and 1.25 mm, the corresponding crack propagation rate is 7.8×10^{-7}, 6.12×10^{-7}, 1.2×10^{-6}, and 1.67×10^{-6} *mm/cycle* respectively. In range of 0.58~0.65 *mm*, crack propagation rate decreases and above 0.65 *mm*, the propagation rate increases proportionally to crack length. However, in case that overload is applied when crack length, a is 0.58 *mm*, crack propagation rate increases from 1.2×10^{-6} to 2.0×10^{-6} *mm/cycle* in range of 0.58~0.65 *mm* and decreases from 2.0×10^{-6} to 7.3×10^{-7} *mm/cycle* in range of 0.65~0.79 *mm* and increases from 7.3×10^{-7} to 1.6×10^{-6} *mm/cycle* in range of 0.79~1.25 *mm*. In other words, crack propagation rate after overload increases and decreases rapidly, and the retardation phenomenon appears over comparatively long range, and then, it becomes similar to the crack propagation

rate in constant amplitude load. Especially, even in the region where crack propagation rate decreases drastically under constant amplitude loading - the transition region from short crack to long crack (the range of crack length a is 0.45~0.65 *mm*)-it can be shown that the crack propagation rate increases drastically after the single overload is applied. There is a region where the crack growth behavior under constant amplitude loading is much different from the behavior after single overload, which is affected by single overload, designated as *ROL*, and the region from the single overload to the point where crack retardation is the greatest is designated as a_r.

Comparison of Fig. 16 and Fig. 17 shows that effective crack stress ratio, U increases drastically after single overload in the range of 0.58~0.65 *mm* where crack propagation rate increases drastically after the single overload. And, U decreases drastically in the range of crack length, a is 0.65~0.79 *mm* where crack propagation rate decreases drastically. In other words, the variation of U after single overload is much the same as the variation of crack growth behavior. From the above results, it can be known that the effective stress range ratio, U provides a significant clue to analyze the crack behavior after the single overload.

The variations of crack propagation rate, da/dN and effective stress range ratio, U according to crack length, a in case of overload applied at $a=1.61$ *mm* are plotted compared with da/dN and U under constant loading in Fig. 18, and Fig. 19. As shown in Fig. 18, under constant amplitude loading as crack length, a increases gradually to 1.61, 1.68, 2.28, and 2.63 *mm*, the crack propagation rate increases 2.36×10^{-6}, 2.39×10^{-6}, 3.57×10^{-6}, and 3.72×10^{-6} *mm/cycle* respectively, while, in case of single overloading, the crack propagation rate is 2.39×10^{-6}, 3.39×10^{-6}, 3.29×10^{-6}, 2.29×10^{-6} and 3.46×10^{-6} *mm/cycle* which shows increase in the range of crack length, 1.61~1.68 *mm*, decrease in the range of 1.68~2.28 *mm*, and increase in the range of 2.28~2.63 *mm*. Also as shown in Fig. 19, as the crack length, a varies to 1.61, 1.68, 2.28, and 2.63 *mm* under constant amplitude loading, U is almost
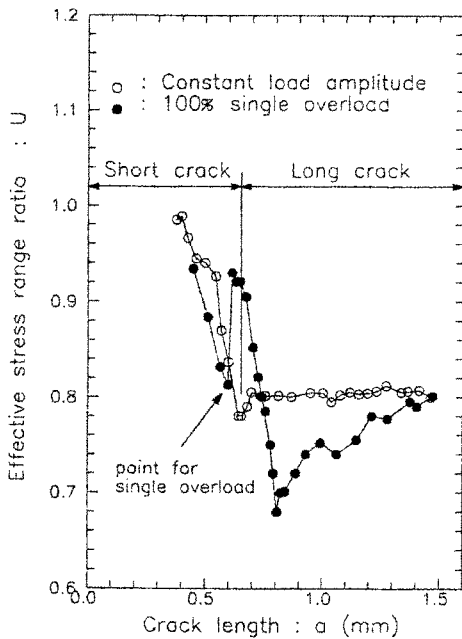

Fig. 17 Comparison of effective stress range ratio for constant load amplitude and 100 % single overload applied at $a=0.58$ mm

Fig. 18 Comparison of crack propagation rate for constant load amplitude and 100 % single overload applied at $a=1.61$ mm
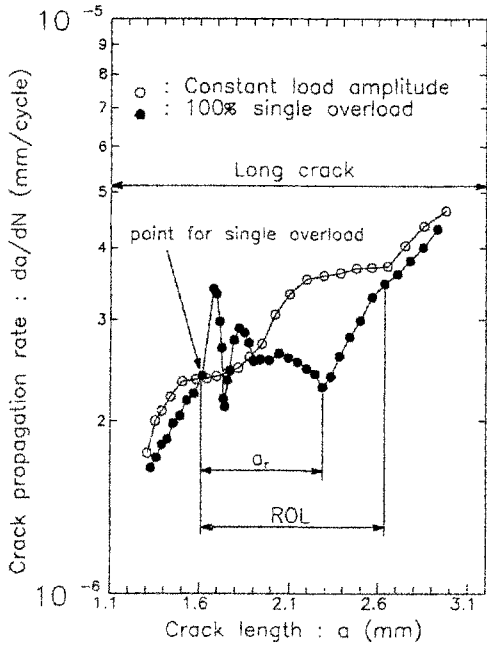

Fig. 20 Comparison of crack propagation rate for constant load amplitude and 100 % single overload applied at $a=3.20$ mm
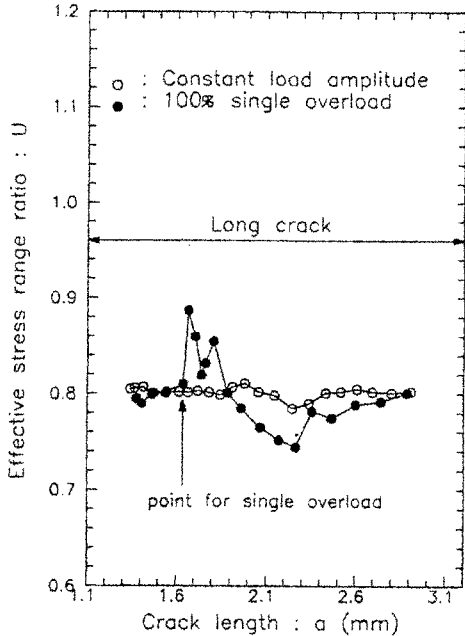

Fig. 19 Comparison of effective stress range ratio for constant load amplitude and 100 % single overload applied at $a=1.61$ mm

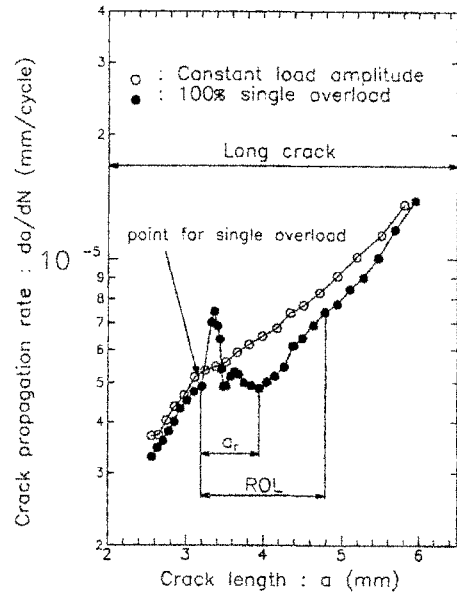constantly 0.8. However, in case of single over-

loading, U is 0.80, 0.87, 0.75, 0.79 sequentially, showing decrease after increase and increase again.

The crack propagation rate, da/dN and effective stress ratio, U after the single overload when crack length is 3.20 mm is compared with those under constant amplitude loading in Fig. 20, and Fig. 21. As shown in Fig. 20, in case of constant amplitude loading as the crack length, a varies to 3.20, 3.36, 3.94, and 4.78 mm, crack propagation rate gradually increases to 5.32×10^{-6}, 5.47×10^{-6}, 6.47×10^{-6}, 8.27×10^{-6} $mm/cycle$ while the propagation rate in case of single overloading, is 4.89×10^{-6}, 7.45×10^{-6}, 4.84×10^{-6} and 7.42×10^{-6} $mm/cycle$ which shows increase in the range of $3.20 \sim 3.36$ mm, decrease in the range of $3.36 \sim 3.94$ mm and increase in the range of $3.94 \sim 4.78$ mm. Also, as shown in Fig. 21, U is almost a constant under constant amplitude loading, but fluctuates such as decrease after increase and increase on case of application of single overload.

To summarize the above results, crack growth just after single overloading is drastically accelerated and decelerated again, appears some retardation range over comparatively long range, and
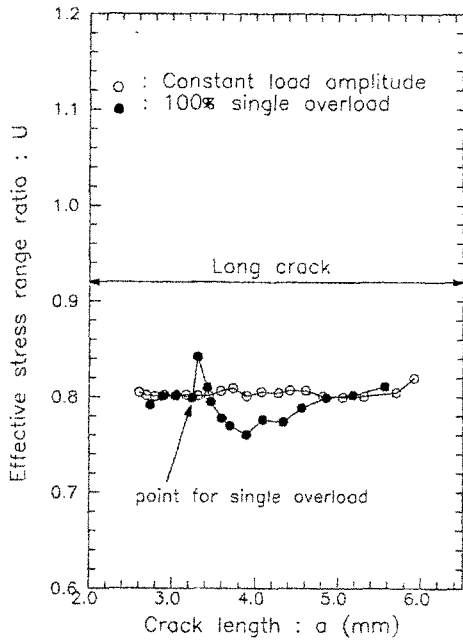
Fig. 21 Comparison of effective stress range ratio for constant load amplitude and 100 % single overload applied at $a=3.20$ mm

then approaches to steady state value. Also, Fig. 18 and Fig. 20 compared with Fig. 19 and Fig. 21 respectively, the crack propagation behavior after single overload is well coherent with the variation of U and this phenomenon is coherent with the results of single overload on short crack (Fig. 16, Fig. 17).

In addition, an abrupt increase and sequential decrease of crack opening stress right after appling single overload was found, and it was consistent with the study (Chermahini et al., 1988) of three-dimensional, elastic-plastic, finite -element analysis of crack closure and opening under cyclic loading with single overload.

3.4 Discussion on the crack growth after the single overload

Several mechanisms of phenomena after overload have been proposed as follows (Ward-Close and Ritchie, 1988) :

(1) Residual stress
(2) Crack closure
(3) Plastic blunting
(4) Crack deflection

(5) Strain hardening

Several mechanisms mentioned above, are proposed to rationalize experimental results, and are correlated with each other except crack deflection effect. Several models to predict fatigue crack growth rate are based on residual stress and crack closure concepts (Ward-Close and Ritchie, 1988) and deformation by residual compression has significant effect on crack closure phenomenon. Residual deformation exists along the wake of fatigue crack suffered previous load history, and will close the crack before the external forces become zero. It can be known that the tendency is well coherent when crack behavior after overload is examined by crack closure concept as in the previous results (Figs. 16~21). In other words, sudden increase of crack growth rate shortly after overload, can be explained by the increase of U, and continuous occurrence of crack retardation can be explained by the decrease of U. Accordingly, crack closure is a significant fracture mechanics parameter in explaining crack behavior under variable load.

There have been various models for explaining crack growth behavior after overload (Wheeler, 1972, Willendorg, et al., 1971). Those models mainly intend to quantify crack growth behavior based on the size of plastic zone developed by overload, which consequently contains many problems (Fleck et al., 1983). Crack growth behavior after overload may be varied by factors of overload ratio, load amplitude, number of overload cycles, time of applying overload, existence of branching crack after overload, type of load, width of specimen, material properties of specimen, and so on (Song and Kwon 1995, Ward-Close and Ritchie 1988). Consequently, it is always problematic to select a single model to assess the effects of overload as well as to evaluate quantitatively crack growth behavior after overload according to the model. It is rather safe to assume that some models might be more suitable for certain conditions. From this perspective, no effort was made to evaluate the effects of overload based on any selected model ; rather, the study results on crack growth behavior after overload were compared with the size of plastic zone after
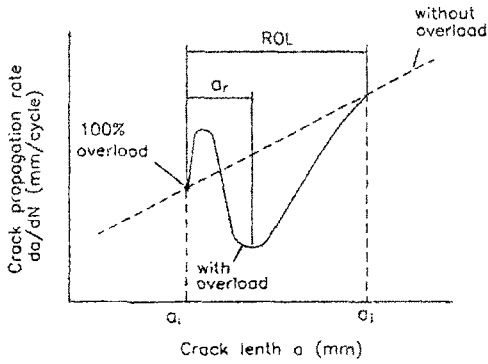
Fig. 22 Schematic illustration of effect of an 100 % single overload on crack growth to calculate promoted or retarded cycles and distance

Table 3 Various phenomena after 100 % single overload

	OL1 (0.58 mm)	OL2 (1.61 mm)	OL3 (3.20 mm)
ROL(mm)	0.68	1.02	1.58
a_r(mm)	0.23	0.67	0.75
ω_{ot}(mm)	0.23	0.50	0.78
N_d(cycle)	Promotion 2.18×10²	Retardation 5.60×10⁴	Retardation 3.79×10⁴
a_d(mm)	Promotion 0.03	Retardation 0.18	Retardation 0.25
N_d/N_f(%)	Promotion 1.14	Retardation 2.93	Retardation 1.98

Fatigue life of constant load amplitude
N_f=1.91×10⁶ cycle

overload as the means to evaluate the effects of overload proposed by researchers previously. The plastic zone size, ω_{ot} by overload is defined as follows (Anderson, 1991).

$$\omega_{ot}=\frac{4K^2}{\pi\beta\sigma_y^2} \qquad (7)$$

Where β is 1 in plane stress state, and 3 in plane strain state. In this study, crack length is observed on the surface of specimen, and the surface is in plane stress state, so β is taken as 1.

In Fig. 22, a_i is the crack length in applying overload, and a_j is the crack length in the effect of overload disappearing. Promoted or retarded cycles N_d by overload are defined as in Eq. (8).

$$N_d = (N_{aj}-N_{ai})_{ot} - (N_{aj}-N_{ai})_{cl} \qquad (8)$$

N_{ai} : Number of cycles to a_i

N_{aj} : Number of cycles to a_j

$(N_{aj}-N_{ai})_{ot}$: Number of cycles between a_i and a_j in case of overload applied

$(N_{aj}-N_{ai})_{cl}$: Number of cycles between a_i and a_j in case of constant amplitude loading

In case of overload applied, promoted or retarded crack length, a_d, is defined in Eq. (9) :

$$a_d=N_d\times\left(\frac{da}{dN}\right)_m \qquad (9)$$

where $\left(\frac{da}{dN}\right)_m$ is mean crack propagation rate in the range from a_i to a_j, and as follows.

$$\left(\frac{da}{dN}\right)_m =\frac{a_j-a_i}{(N_{aj}-N_{ai})_{cl}} \qquad (10)$$

Various phenomena after overload applied are listed in Table 3 with respect to 3 cases of overload, where OL1, OL2, and OL3 are overload applied at crack length 0.58 mm, 1.61 mm, and 3.20 mm respectively. The range of a_r where crack propagation rate by overload shows great difference from that of under constant amplitude loading and is retarded, coincide with plastic zone size, ω_{ot}. It is known from this that the retardation becomes most severe at the point just over the plastic zone generated by overload. In the size of ROL affected by overload, OL1 is 3 times as much as the plastic zone size of overload, while OL2 and OL3 are about 2 times. Also, actually, crack retardation does not always occur, but it can be known that crack grows fast in cases of OL1, and crack growth is retarded by 0.18 mm and 0.25 mm in cases of OL2 and OL3 respectively compared with constant amplitude load. The corresponding number of cycle is within 3 % of the whole fatigue life.

4. Conclusion

With pre-cracked plane specimen and hole defected specimen, short crack and long crack behaviors and the crack behaviors after the overload are examined by using crack opening behavior under out of plane bending loading. Elas-

tic compliance method using strain gage, which is precise and capable of much data continuously, is used to measure crack opening stress.

(1) As short crack propagates faster than long crack under the same stress intensity factor range, it can not be defined by the previous fracture mechanical parameter, and the short crack characteristics are shown until crack length becomes to 0.65 mm. The material constants of the Paris' equation for long crack, C and m are 2.46×10^{-9}, 3.60 and ΔK_{th} is about 3 $MPa\sqrt{m}$ respectively.

(2) The result with respect to the crack propagation rate arranged by effective stress intensity factor range, shows that linear relation holds in short crack, which means that short crack growth behavior can be quantitatively expressed by a fracture mechanics parameter employing effective stress intensity factor range. The material constants of the Paris' equation using effective stress intensity factor range, C' and m' are 8.38^{-9} and 3.41, respectively.

(3) Comparing the crack behavior after the overload with that on the constant amplitude loading shows that crack propagation rate increases and decreases rapidly, and the retardation phenomenon appears over comparatively long range, and then, it becomes similar to the crack propagation rate in constant amplitude load. This phenomenon is common in both short crack and long crack, and can be explained by effective stress range based on crack opening behavior.

(4) The range where the maximum retardation occurs after the overload, is well coherent with the size of plastic zone formed by the single overload. From this result, it can be known that the maximum retardation occurs at the boundary of the plastic zone after the overload. Also, the range affected by the single overload is more than 2 times as large as the size of the plastic zone. and the number of cycles promoted or retarded is within 3% of the total fatigue life.

References

Anderson, T. L., 1991, *Fracture Mechanics-Fundamentals and Applications*. CRC Press, Boston, pp. 620~629.

Annual Books of ASTM Standards, Vol. 03.01, E647-91, 1991, "Standard Test Method for Measurement of Fatigue Crack Growth Rates," pp. 674~701.

Annual Books of ASTM Standards, Vol. 03. 01, E740-88, 1988, "Standard Practice for Fracture Testing With Surface-Crack Tension Specimens." pp. 689~696.

Chermahini, R. G., Shivanumar, K. N., Newman, J. C., Jr., 1988, "Three-Dimensional Finite-Element Simulation of Fatigue Crack Growth and Closure," *Mechanics of Fatigue Crack Closure*, ASTM STP 982, pp. 398~413.

Elber, W., 1971, "The Significance of Fatigue Crack Closure," *Damage Tolerance in Aircraft Structures*, ASTM STP 468, pp. 230~242.

Fleck, N. A., Smith, I. F. and Smith R. A., 1983, "Closure Behavior of Surface Crack," *Fatigue and Engineering Materials and Structures*, Vol. 6, No. 3, pp. 225~239.

Gan, D. and Weertman, J., 1983, "Fatigue Crack Closure after Overload," *Engineering Fracture Mechanics*, Vol. 18, No. 1, pp. 155~160.

Kurihara, M., Katoh, A. and Kawahara, M., 1987, "Effects of Stress Ratio and Step Loading on Fatigue Crack Propagation Rate," *Current Research on Fatigue Cracks, Current Japanese Materials Research*, Vol. 1, pp. 247~265.

McEvily, A. J., 1988, "On Crack Closure in Fatigue Crack Growth," *Mechanics of Fatigue Crack Closure*, ASTM STP 982, pp. 35~43.

Park, J. H., Song, J. H., Earmme, Y. Y., Kim, C. Y. and Kang, K., J., 1988, "Personal Computer-Based Fatigue Testing Automation and Improvement in Fatigue Behavior Monitoring," *Transactions of the KSME*, Vol. 12, No. 1, pp. 123~130.

Perez, R., Grandt, A. F. Jr and Saff, C. R., 1990, "Tabulated Stress-Intensity Factors for Corner Cracks at Holes Under Stress Gradients," *Surface-Crack Growth : Models, Experiments, and Structures*. ASTM STP 1060, pp. 49~62.

Schijve, J., 1981, "Some Formulas for the Crack Opening Stress Level," *Engineering Fracture Mechanics*, Vol. 14, pp. 461~465.

Song, S. H. and Kim, J. B., 1995, "Analysis of

Stress Distribution around Defects and Inclusions by F. E. M.," *KSME Journal*, Vol. 9, No. 3, pp. 351~359

Song, S. H. and Kwon, Y. K., 1995, "A Study on Crack Retardation Behavior by Single Overload," *Transaction of the KSME*, Vol. 19, No. 2, pp. 451~462.

Song, S. H. and Won, S. T., 1985, "Behavior of Initiation and Propagation of Fatigue Crack under Periodic Overstressing (I)," *Transactions of the KSME*, Vol. 9. No. 3, pp. 301~308.

Stephens, R. I., Chen, D. K. and Hom, B. W., 1976, "Fatigue Crack Growth with Negative Stress Ratio Following Single Overloads in 2024-T3 and 7075-T6 Aluminum Alloy," ASTM STP 595, pp. 27~40.

Suresh, S. and Ritchie, R. O., 1984, "Propagation of Short Fatigue Cracks," *International Metals Reviews*, Vol. 29, No. 6, pp. 445~476.

Ward-Close, C. M. and Ritchie, R. O., 1988, "On the Role of Crack Closure Mechanisms in Influencing Fatigue Crack Growth Following Tensile Overloads in a Titanium Alloy : Near Threshold Versus Higher ΔK Behavior," *Mechanics of Fatigue Crack Closure*, ASTM STP 982, pp. 93~111.

Wheeler, O. E., 1972, Spectrum Loading and Crack Growth. *J. Basic Eng., Trans. ASME*, Series D94(1), pp. 181~186.

Willenborg, J., Engel, R. M. and Wood, H. A., 1971, "A Crack Growth Retardation Model Using an Effective Stress Concept," WPAFB, TM-71-1-FBR.

Yamada, K., Shimizu, M. and Kunio, T., 1987, "Threshold Behavior of Small Cracks in Dual Phase Microstructures." *Current Research on Fatigue Cracks, Current Japanese Materials Research*, Vol. 1, Elsevier Applied Science, New York, pp. 27~40.